Preparation and Surface Structure of Nanocrystalline Cadmium Sulfide (Sulfoselenide) Precipitated from Dimethyl Sulfoxide Solutions

Rivka Elbaum,[†,‡] Shimon Vega,*[,†] and Gary Hodes*[,‡]

Departments of Chemical Physics and of Materials and Interfaces, Weizmann Institute of Science, Rehovot 76100, Israel

Received July 14, 2000. Revised Manuscript Received April 11, 2001

We present a method for the synthesis of CdS and CdS_xSe_{1-x} nanocrystals by precipitation from a solution of cadmium carboxylate in dimethyl sulfoxide (DMSO) with or without elemental S (Se). The reaction in the presence of hydrazine has also been investigated. The CdS particle size, determined by X-ray diffraction, varied between 2 and 7 nm, depending on the reaction conditions. The CdS_xSe_{1-x} crystal size varied between 5 and 10 nm. UV spectra of the particles showed an increase of the optical band gap as the size of the crystals decreased. The surface structure of the CdS nanocrystals was characterized by IR and NMR spectroscopy. The spectra of CdS particles prepared with cadmium acetate and sulfur showed four types of binding sites at the crystallite surfaces: oxidized sulfur, acetate adsorbed to the surface cadmium in a bridging complex, oxygen-bound DMSO, and hydroxyl ions.

Introduction

Many synthetic methods for the preparation of nanocrystalline semiconductor powders, in particular of binary sulfide and selenide complexes, have been reported. The most straightforward one is a simple precipitation of these nanoparticles from aqueous solutions of metal salts and sulfide or selenide. This technique usually leads to crystals with sizes on the order of 5 nm but with surface properties that can vary considerably. Of the few surface structural studies carried out to date, most have involved thiol-capped nanoparticles.[1−3] Extended X-ray absorption fine structure (EXAFS) studies of nanocrystalline CdS precipitated from a dimethylformamide solution elucidated the binding between CdS and the solvent and of excess Cd or S ions on the CdS surface.[4] NMR studies have shown that CdS, precipitated from an aqueous solution of Cd salt and sodium sulfide, exhibits different surface chemistries depending on the ratio between Cd and sulfide concentrations.[5] Semiconductor properties are normally very sensitive to surface effects: for nanocrystalline semiconductors, with very large surface-to-volume ratios, these effects are even more pronounced.[6]

Films of nanocrystalline semiconductors can be electrodeposited from dimethyl sulfoxide (DMSO) solutions of metal salts and elemental S or Se.[7] During investigations of this process, it was noticed that only a limited range of anions of the metal salts can be used, because many anions cause direct reaction of the metal with the chalcogen. In particular, if cadmium carboxylates are used in the electrodeposition of CdS, most of the Cd precipitates in solution as CdS in the absence of an applied potential.

In the present study we investigate this precipitation reaction and characterize the nanocrystalline products. Because the surface properties of such nanocrystals may be expected to be different from those precipitated in aqueous solutions, the chemistry of the surfaces is also studied, using IR and NMR spectroscopies.

Experimental Section

Synthetic Methods. CdS nanocrystals were synthesized by dissolving elemental S to final concentrations varying between 5 and 160 mM in DMSO at 90 °C for about 1 h. This solution was heated to the reaction temperature, ranging between 100° and 150 °C, and a preheated solution of cadmium acetate ($CdAc_2$) or cadmium formate ($CdFor_2$) in DMSO was added, reaching final concentrations between 5 and 240 mM or 20 and 140 mM, respectively. The solution became lemon-yellow after several minutes, and its color stabilized within 10 min. The reaction solution was cooled to ambient temperature after about 1 h. A powder of CdS was extracted by adding acetone (or methanol) to the solution and centrifuging, collecting the precipitant, and repeating this process two more times. After evaporation of the acetone (or methanol) at room temperature, a dry CdS powder was obtained which had a yield of 50−60% of the more dilute species in the solution.

$CdSe_xS_{1-x}$ samples were prepared by dissolving 5 mM (final concentration) elemental Se in DMSO at 150−160 °C. This solution was brought to the reaction temperature, between 120 and 170 °C, and a preheated solution of $CdAc_2$ or $CdFor_2$ in DMSO was added that resulted in final concentrations of 5 mM or 5−10 mM, respectively. After 1−6 h the solution was

* To whom correspondence should be addressed.
† Department of Chemical Physics.
‡ Department of Materials and Interfaces.

(1) Sachleben, J.; Wooten, E.; Emsley, L.; Pines, A.; Colvin, V.; Alivisatos, A. *Chem. Phys. Lett.* **1992**, *198*, 431.
(2) Rockenberger, J.; Tröger, L.; Rogach, A.; Tischer, M.; Grundmann, A.; Eychmüller, A.; Weller, H. *J. Chem. Phys.* **1998**, *108*, 7807.
(3) Winkler, U.; Eich, D.; Chen, Z. H.; Fink, R.; Kulkarni, S. K.; Umbach, E. *Chem. Phys. Lett.* **1999**, *306*, 95.
(4) Hosokawa, H.; Fujiwara, H.; Murakoshi, K.; Wada, Y.; Yanagida, S.; Satoh, M. *J. Phys. Chem.* **1996**, *100*, 6649.
(5) Ladizhansky, V.; Hodes, G.; Vega, S. *J. Phys. Chem. B* **1998**, *102*, 8505.
(6) Alivisatos, A. P. *J. Phys. Chem.* **1996**, *100*, 13226.
(7) Hodes, G. *Isr. J. Chem.* **1993**, *33*, 95−106.

10.1021/cm0005790 CCC: $20.00
Published on Web 06/02/2001

cooled to ambient temperature. Powders were extracted from the solution by the acetone precipitation procedure described above. To form mixed crystals of CdS_xSe_{1-x} with varying stoichiometries, S was added to the Se solution, reaching a total concentration of 5 mM chalcogen.

Precipitation of CdS, without adding elemental chalcogen, was accomplished by refluxing 100 mM $CdAc_2$ in DMSO at 140 or 180 °C for several hours. The powder was extracted by the same acetone precipitation procedure. This reaction proceeds very slowly at room temperature: A 170 mM solution of $CdAc_2$ in DMSO resulted in a yellow solution only after several months.

CdS was precipitated by sonochemistry when 100 mM Cd salt {$CdAc_2$ or $CdCl_2$} in DMSO was sonicated at room temperature with a titanium sonic probe (Ultrasonic liquid processor VC-600, 20 kHz, Sonics & Materials operated at 30 W in continuous mode) for 1 h. The steady-state temperature of the sonicated solution was 65−75 °C.

For the hydrazine-based synthesis, hydrazine (ca. 1 mL of hydrazine hydrate to 25 mL of a DMSO solution) was added to ca. 5 mM Se in DMSO followed by a slightly greater than stoichiometric amount of $CdAc_2$ in DMSO.

Characterization Methods. Powder X-ray diffraction (XRD) spectra were obtained on a Rigaku RU-200 B Rotaflex diffractometer using Cu Kα radiation. The acceleration voltage was 45 kV with a 150 mA current flux. Scatter and diffraction slits of 0.5 mm and collection slits of 0.3 mm were used. XRD was taken of the powders attached to a glass slide by double-sided sticky tape. Data were collected for 2θ in the range of 15−60°, with a counting rate of 0.30°/min and a sample interval of 0.020°.

Transmission electron micrographs were taken on a Philips EM-400 operating at 100 kV. A drop of the reaction solution was placed on a carbon-coated copper grid and most of the liquid removed by wick action after a few minutes.

UV measurements were performed on a Jasco V-570 spectrometer. Spectra were measured at 400 nm/min at 1 nm resolution. The optical transmittance of the reaction solution and of the powder, solvated in DMSO, was measured over the range of 1000−250 nm in a quartz cuvette. The value of the optical band gap was estimated to be equal to the point where the transmission was two-thirds of its value at the onset of the decrease.[7]

IR spectroscopy was carried out on a Bruker Ifs66 Fourier transform infrared (FTIR) spectrophotometer in the single beam absorbance mode over the range of 400−5000 cm^{-1}. The number of scans was 100−200 at a scan velocity of 40 kHz and with a slit of 1 mm. The sample chamber was purged with nitrogen. The optical transmission was measured on pellets prepared from a mixture of 2 mg of semiconductor powder and 150 mg of KBr (Merck for IR spectroscopy) pressed at 10 atm.

NMR spectra were measured on a Bruker DXP 300 MHz spectrometer. ^{113}Cd NMR spectra were obtained from samples rotating in the external magnetic field at the magic angle, by Fourier transformation of the free induction decay (FID) signal starting at the echo position of a spin−echo experiment ($\pi/2-\tau-\pi-\tau$), or appearing after the mixing time of a cross-polarization magic angle spinning (CPMAS) experiment. ^{13}C spectra were obtained by CPMAS experiments and ^{1}H MAS spectra from FID signals that were detected after a single 90° excitation pulse. The spinning frequency of the samples during ^{113}Cd and ^{13}C NMR measurements was equal to 3.5 kHz. For the proton spectra this frequency was 9 kHz. Samples were prepared by inserting 100−150 mg of the powders in a 4 mm Bruker rotor.

T_2 relaxation time values of ^{113}Cd in CdS samples were measured by monitoring echo signal intensities as a function of τ in spin−echo experiments. These τ values were incremented with time intervals that were equal to the spinning period.

Results and Discussion

XRD and UV Spectroscopy of CdS. The reaction of S with $CdAc_2$ in DMSO for the synthesis of CdS nanocrystals required typically about 10 min to reach completion, depending on temperature. With $CdFor_2$, a stronger reducing agent than acetate (see the reaction mechanism below), the reaction took only a few minutes. The CdS precipitates were first studied by XRD in order to establish their crystal structure (zinc blende or wurtzite) and particle size. Figure 1 shows XRD patterns of CdS precipitated from $CdAc_2$ in DMSO at three different temperatures (Figure 1a−c), together with a reference spectrum of a commercial sample of bulk wurtzite CdS (Figure 1d). In our case the CdS precipitates had a predominantly wurtzite structure. This can be clearly seen by the triplets, centered around 27° in parts b and c of Figure 1 of particles synthesized at 130 and 150 °C, respectively, and is inferred from the width of the peaks in Figure 1a of particles synthesized at 100 °C. The coherence lengths of the particles, derived from the high angle peaks, are given in Table 1. The precipitate formed from $CdFor_2$ at 120 °C, on the other hand, exhibited a predominantly sphalerite phase (Figure 1e).

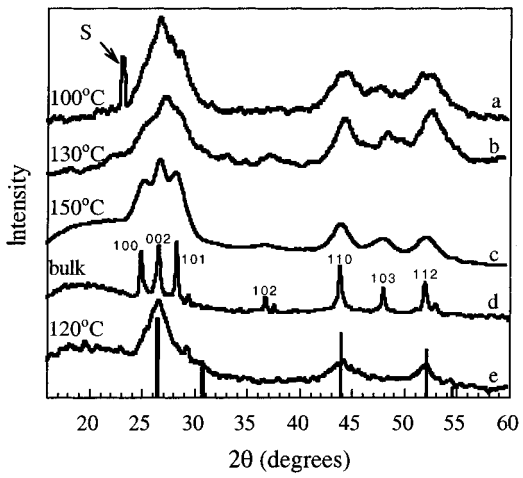

Figure 1. XRD spectra of CdS nanoparticles synthesized from $CdAc_2$ at temperatures (a) 100, (b) 130, and (c) 150 °C compared with the spectra of (d) a bulk CdS powder and of (e) CdS prepared from $CdFor_2$ and sulfur at 120 °C.

Table 1. Comparison between UV and XRD Data of CdS Nanoparticles

preparation temp (°C)	band gap measured from absorption spectra	diameter from XRD line width (nm)
100[a]	2.62 eV (472 nm)	4.0
130[a]	2.58 eV (480 nm)	5.5
150[a]	2.56 eV (483 nm)	6.6
120[b]	2.55 eV (487 nm)	5.3

[a] Prepared from the $Cd(Ac)_2$ wurzite phase. [b] Prepared from the $Cd(For)_2$ zinc blende phase.

A transmission electron microscopy (TEM) micrograph of a precipitate formed at 100 °C is shown in Figure 2. Although the individual particles are aggregated into larger ones, the individual particles can be distinguished and are typically 4−5 nm in size, in agreement with the XRD results.

The precipitates can be redissolved in DMSO as colloidal sols. Optical absorption spectroscopy of these sols was used to measure the band gaps of the various precipitates. Because the crystal sizes are in the quantum size regime, a decrease in size results in an increase in the band-gap energy. The band-gap values calculated from these spectra are also given in Table 1.

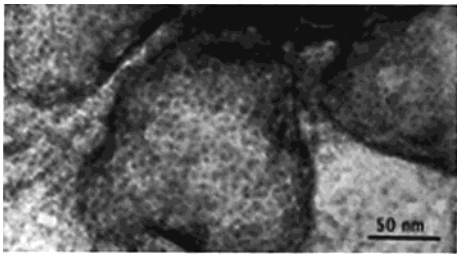

Figure 2. TEM micrograph of a CdS precipitate prepared from $CdAc_2$ + S in DMSO at ca. 100 °C.

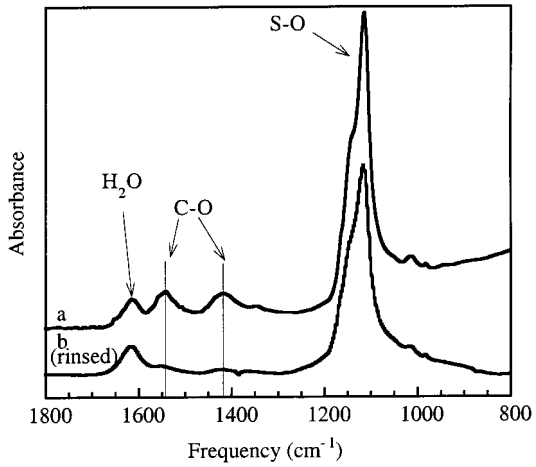

Figure 3. IR spectra of a nanocrystal CdS powder sample as synthesized from $CdAc_2$ and S in DMSO (a) after rinsing in acetone and (b) after additional rinsing of the particles with water.

IR Spectroscopy. Surface properties of CdS nanocrystalline powder samples, prepared at 120 °C from a solution of $CdAc_2$ and S in DMSO, were studied by IR and NMR spectroscopies. IR spectra of these samples are very sensitive to surface species, because pure CdS does not show any IR absorption.[8]

The strongest features in the IR spectrum are the S−O stretching bands between 1190 and 1060 cm^{-1}, either of DMSO or of oxidized sulfur in the sample. Figure 3 shows these S−O peaks as well as the carboxyl symmetric (1416 cm^{-1}) and antisymmetric (1545 cm^{-1}) stretching bands of the acetate group. The water bending mode is observed at 1613 cm^{-1}. A significant decrease in the intensities of the carboxyl peaks, and to a lesser extent of the S−O peaks, was observed after rinsing the sample with water. This indicates a change in the surface structure and suggests that part of the sulfate and acetate groups bound to the surface are removed by water.

A comparison of the carboxyl signal of the nanocrystals with that of commercial $CdAc_2 \cdot 2H_2O$ shows a shift of 13 cm^{-1} of the antisymmetric stretching band. This shift can be interpreted as bonding between the carboxyl and the nanocrystal surface. Additionally, the absence of a signal equivalent to $CdAc_2 \cdot 2H_2O$ indicates that there is no acetate, which is not surface-bound, dissolved in solution (as might occur in voids between crystals). The difference between the stretching vibrations of carboxyl in $CdAc_2 \cdot 2H_2O$ (at 1558 and 1416 cm^{-1}) and of acetate on the surface of CdS nanocrystals (at 1545 and 1416 cm^{-1}) is demonstrated in Figure 4. The difference between the symmetric and antisymmetric stretching energies seems to be characteristic for a bridging complex,[9] in agreement with the adsorption data of benzoic acid on a CdSe surface.[10]

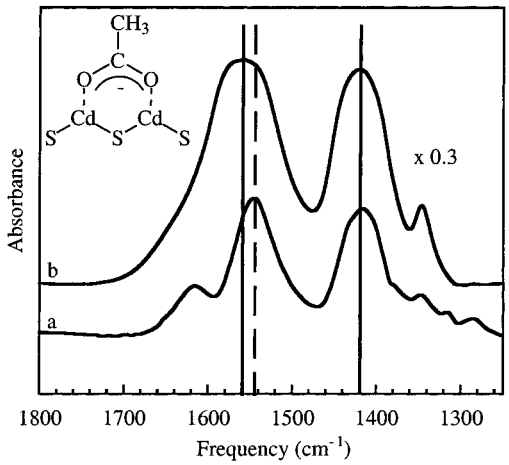

Figure 4. Carboxyl stretching bands of (a) an as-synthesized CdS sample and of (b) a commercial $CdAc_2 \cdot 2H_2O$ (0.3% $CdAc_2 \cdot 2H_2O$ in KBr) sample. The inset shows the bridging complex of the acetate ion.

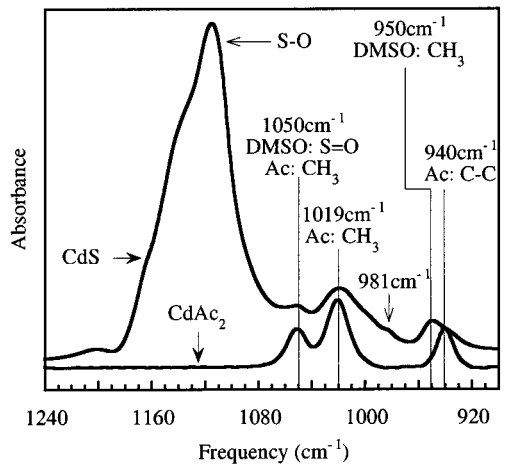

Figure 5. Range of 1240−900 cm^{-1} of the IR spectrum, showing the S−O peaks of DMSO in a CdS nanocrystal and the CH_3 and C−C bands in a commercial sample of $Cd(Ac)_2 \cdot 2H_2O$ (0.3% $CdAc_2 \cdot 2H_2O$ in KBr). The assignments of the peaks are 1050 cm^{-1} for the DMSO S=O stretching and the acetate CH_3 rocking, 1019 cm^{-1} for the acetate CH_3 rocking, 950 cm^{-1} for the DMSO CH_3 rocking, and 940 cm^{-1} for the acetate C−C stretching. The peak at 981 cm^{-1} is related to O-bonded DMSO.

The coordination of DMSO to Cd changes its S−O bond energy as shown in the following:[11]

$$\underset{\text{S coordination}}{1240\ cm^{-1}} \leftarrow \underset{\text{free molecule}}{1050\ cm^{-1}} \rightarrow \underset{\text{O coordination}}{915\ cm^{-1}}$$

In Figure 5, the 920−1240 cm^{-1} region of the IR spectra of $CdAc_2 \cdot 2H_2O$ and of the CdS sample is shown. The peak of free DMSO (at 1050 cm^{-1}) overlaps with a

(8) Kizilyalli, M.; Biligin, M.; Usanmaz, A. *J. Solid State Chem.* **1989**, *80*, 75.

(9) Nakamoto, K. *Infrared and Raman Spectra of Inorganic and Coordination Compounds*; Wiley-Interscience:New York, 1978; p 232.

(10) Bruening, M.; Moons, E.; Cahen, D.; Shanzer, A. *J. Phys. Chem.* **1995**, *99*, 8368.

(11) Cotton, F. A.; Francis, R.; Horrocks, W. D., Jr. *J. Phys. Chem.* **1960**, *64*, 1534.

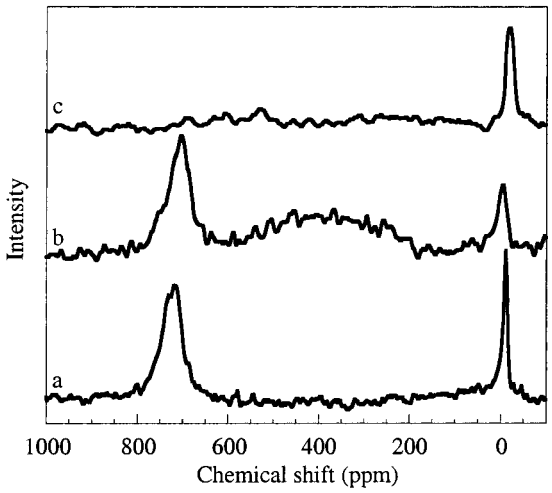

Figure 6. ^{113}Cd NMR spectra of a CdS sample that was synthesized a few days before the measurement, resulting from (a) a spin−echo experiment, with a repetition time of 150 s and 1080 accumulations, and (b) a CPMAS experiment, with a repetition time of 4 s and 32 000 accumulations. This CPMAS result is compared to (c) the spectrum of a similar experiment, with a repetition time of 30 s and 32 000 accumulations, on a CdS sample, that was prepared 1 year prior to the experiment. CP mixing times were 5−10 ms.

peak of $CdAc_2 \cdot 2H_2O$. Thus, we cannot make any conclusions about the relative amount of free DMSO in the nanoparticle sample. A small shoulder at 981 cm^{-1} in the spectrum of the CdS sample may be related to oxygen-bonded DMSO. The acetate C−C stretching peak at 940 cm^{-1} overlaps with the DMSO methyl rocking peak at 950 cm^{-1}, and the S-coordinated DMSO peak, if at all present in the spectrum, overlaps with the main S−O peak and cannot be resolved.

To conclude this section, the IR spectra indicate that carboxylate groups bind to the particle surface in the bridging complex and that DMSO molecules bind through O bonding.

NMR Spectroscopy. The surface investigation was completed by a set of ^{113}Cd, ^{13}C, and ^{1}H NMR experiments. In Figure 6, ^{113}Cd MAS spectra of a CdS nanocrystal sample are shown that were obtained (a) from a spin−echo experiment and (b and c) from CPMAS experiments. The first experiment results in spectral lines for all types of ^{113}Cd atoms in the sample, provided that their T_1 relaxation times are shorter than the repetition time of the signal acquisition. The CP-MAS experiments result in spectra containing lines only of those ^{113}Cd atoms that can be polarized by their neighboring hydrogen nuclei.

The spin−echo experiment shows two lines at 719 and −7 ppm. On the basis of the reported chemical shift of bulk CdS at 687 ppm,[12] the line at 719 ppm was assigned to cadmium fully coordinated to sulfur (Cd−S). Cadmium salts of carboxylic acids show ^{113}Cd chemical shifts between −53 and 20 ppm,[12] while $CdAc_2 \cdot 2H_2O$ has a ^{113}Cd shift of −53 ppm. In accordance with the IR results showing the bonding of acetate to surface cadmium, we assign the line at −7 ppm to surface ^{113}Cd coordinated to acetate (Cd−Ac).

(12) Duncan, T. M. *A Compilation of Chemical Shift Anisotropies*; Farragut Press: Chicago, 1990.

The integrated intensity of the Cd−Ac line at −7 ppm in Figure 6a is about 60% that of the Cd−S peak at 719 ppm. Between 20 and 40% (depending on the crystal size) of the cadmium atoms are expected to be surface atoms in our nanocrystalline samples. Although the spectrum in Figure 6a is obtained by a spin−echo experiment, the relative intensities of its two lines do not necessarily resemble the ratios between the relative quantities of bulk and surface cadmium in the sample. This is due to the fact that cadmium atoms in CdS can experience a broad distribution of T_1 values. Bulk CdS material has a T_1 of about 200 s and nanosized material that of about 70 s,[5] which are both on the order of the experimental repetition times, with ∼150 s between acquisitions.

The width of the Cd−S line at 719 ppm is 3300 Hz, which corresponds to a transverse relaxation time T_2* of 95 μs. The spin−echo T_2 value of this line is larger than 500 μs, indicating that the Cd−S line is composed of a set of lines with different chemical shifts. They may correspond to Cd atoms that are coordinated to four S atoms inside the particles or that are parts of surface species such as S-bound Cd−DMSO and Cd−SO_x. The Cd−Ac signal at −7 ppm is narrow, with a line width of 716 Hz and a T_2* of 444 μs. Its spin−echo T_2 value is of the same order, suggesting that only one type of cadmium to acetate bond exists on the surface.

The ^{113}Cd CPMAS spectrum in Figure 6b was obtained from a sample that was synthesized a week before the NMR measurement, while Figure 6c presents a CPMAS spectrum of a sample that was prepared a year before the NMR measurement and was kept during that time at room temperature. To ensure that only ^{113}Cd atoms close to protons are observed, a repetition time much shorter than the relaxation time of Cd in bulk CdS was used. The broad band between 600 and 200 ppm in Figure 6b can be attributed to a large variety of ^{113}Cd atoms bound to oxygen (Cd−O) on the surface,[5] including cadmium coordinated to DMSO via oxygen. Different oxidation states of the cadmium can give rise to many lines that merge together into this broad band. This band is missing in the spin−echo spectrum, probably because of its long overall cadmium T_1 values. The large relative integrated intensity of this band indicates that a large part of the surface is oxidized, presumably more than the part coordinated to acetate.

The line at 719 ppm in Figure 6b is ascribed to fully sulfur coordinated cadmium atoms that are close to the surface. These atoms are near protons and can still be bulklike species, such as surface Cd, that are bound to sulfur oxides or to DMSO via their sulfur atoms. This Cd−S as well as the Cd−O lines are missing in the CPMAS spectrum of the older sample.

To investigate the disappearance of these species, proton spectra were collected of three samples that were prepared at different times prior to the NMR measurements. The proton spectrum of the sample that was prepared a few days before the NMR experiment (Figure 7a) shows two intense lines, one of water (5.18 ppm) and the other of hydroxyl groups (2.75 ppm). Comparing this spectrum with spectra of samples prepared 1 month and 1 year prior to the experiments (Figure 7b and 6c) shows that the intensity of the hydroxyl line decreases during aging, meaning that the concentration of the

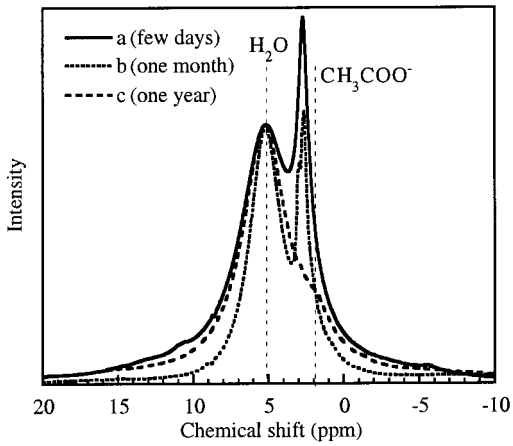

Figure 7. ^{1}H MAS spectra of CdS samples, prepared (a) a few days before, (b) 1 month before, and (c) 1 year before the date of the NMR experiments. The position of the methyl line of $CdAc_2 \cdot 2H_2O$ is marked in the spectrum, as well as the position of the water line. These spectra were recorded after a single 90° excitation pulse.

hydroxyl groups on the surface of the nanoparticles decreases. Hence, we conclude that the $^{113}Cd-O$ band in Figure 6b that is missing from the older sample in Figure 6c corresponds to Cd nuclei that are excited by OH protons on the surface.

After the sample was washed with acetone (in which cadmium acetate is insoluble), two centerbands at −53 and −66 ppm appeared in the CPMAS spectrum, both with a set of strong sidebands. These spectral features are identical with those of a CdS sample mixed with pure $CdAc_2 \cdot 2H_2O$. The signal at −53 ppm was therefore assigned to pure $CdAc_2 \cdot 2H_2O$, and the line at −66 ppm corresponds to a new type of Cd that is produced by some bonding between $Cd(CH_3COO)_2 \cdot 2H_2O$ and one of the components in the CdS sample. We attribute this to the coordination of Cd to the remains of DMSO in the powder. Checking the ^{13}C CPMAS spectrum of the mixed sample, we found a new line at 42.7 ppm, close to the chemical shift of DMSO (at 43 ppm[12]), supporting our assumption. The formation of $CdAc_2 \cdot 2DMSO$ crystals was already reported by Glavas and Ribar.[13] Because the cadmium line of the complex shows sidebands, we believe that crystals of this complex are formed. This complex may play a role in the formation of the CdS crystallites; however, there is no direct indication that there exists a connection between its formation and the particle surface structure.

The strong water line in the proton spectrum in Figure 7 suggests that water molecules are occluded between the particles. With the disappearance of the OH line in the spectrum of the older sample, two additional lines can be distinguished, one at 2.93 ppm and one at 1.90 ppm. The line at 2.93 ppm decreases together with the OH line. This line can be assigned to the methyl proton line of DMSO, shifted by 0.42 ppm from pure DMSO (at 2.53 ppm[14]). This shift may be due to the formation of the complex between DMSO and cadmium. O-bonded DMSO shows an increase in its methyl chemical shift up to 3.05 ppm, while S-bonded

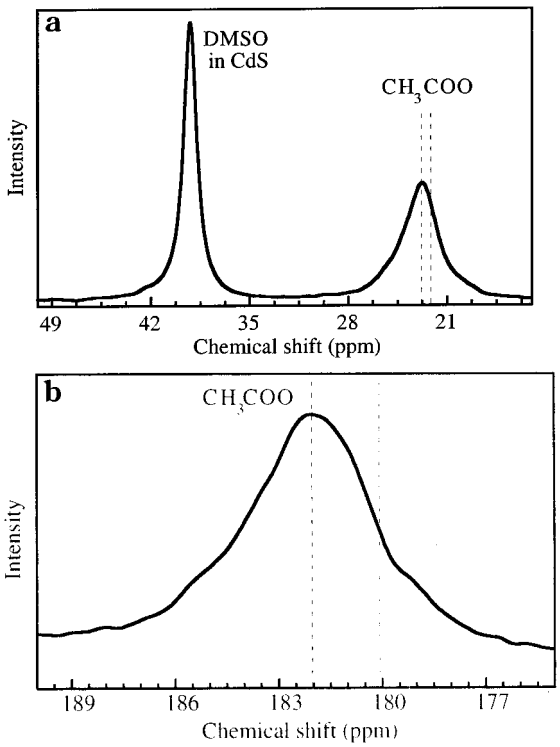

Figure 8. (a) Methyl and (b) carboxylate regions of ^{13}C CPMAS NMR spectra of CdS nanocrystals. The CP mixing time of these experiments was 2 ms, and the repetition delay was 4 s. A total of 12 000 FID signals were accumulated and Fourier transformed. The carboxylate spectrum is 3.4 times enhanced with respect to the methyl spectrum.

DMSO has a shift at around 3.5 ppm.[14] In our case the shift agrees better with O-bonded DMSO. This is consistent with the IR measurement that showed a small amount of O-bonded DMSO and with the fact that cadmium salts tend to form O-bonded complexes.[14] The small line at 1.9 ppm corresponds to the methyl groups of acetate ions in the sample.

To extend our knowledge about the surface structure of the nanoparticles, ^{13}C CPMAS spectra were measured. These are shown in Figure 8. The assignments of the lines were made according to chemical shift values found in the literature.[12] The DMSO line at 39.4 ppm is shifted from free DMSO by −3.6 ppm. The DMSO molecules either are confined in pores between the particles or are bound to the particle surfaces. In both cases a change in the chemical shift can be expected.

To characterize the acetate binding to the surfaces of the nanoparticles, a ^{13}C CPMAS spectrum of pure $CdAc_2 \cdot 2H_2O$ was measured and compared with the ^{13}C CPMAS spectrum of a CdS sample. The first spectrum exhibits two lines for the acetate group, separated by 1.9 ppm, and two lines for the methyl group with a splitting of 0.8 ppm. The positions of the two methyl and carboxyl lines are marked by the dotted lines in the spectrum of the CdS sample in Figure 8. The line splittings in the $CdAs_2 \cdot 2H_2O$ spectrum are a result of the fact that the acetate ions are situated in two nonsymmetry-related lattice positions in the crystal. Both acetate ions form a bidentate bonding to the cadmium atom in the unit cell, but one of them also bridges to a second cadmium outside its unit cell. The acetate group that forms this bridging shows a carboxylic signal at 182.0 ppm and a methyl signal at 22.8 ppm.

(13) Glavas, M.; Ribar, T. *Croat. Chem. Acta* **1967**, *39*, 253.
(14) Davis, J. D. In *Advances in Inorganic Chemistry and Radiochemistry*; Emeleus, A. G. S., Ed.; Academic Press: Cambridge, England, 1981; Vol. 24, p 115.

Table 2. Summary of the Surface Analysis by NMR and IR

type of bond	detection method	frequencies
Cd−S	^{113}Cd NMR	709 ppm
Cd−S−OH	^{113}Cd NMR	709 ppm
Cd−Ac	IR	1545 cm^{-1}
	^{13}C NMR	182 ppm
Cd−OH	^{113}Cd NMR	200−600 ppm
	^{1}H NMR	2.75 ppm
(DMSO)−O−Cd	IR	981 cm^{-1}
	^{1}H NMR	3.93 ppm
S−O	IR	1190−1060 cm^{-1}

The acetate group that does not form the bridging results in a carboxyl line at 180.1 ppm and a methyl signal at 22.0 ppm.[15] The spectrum of the nanocrystals shows broad lines with maxima at the chemical shift values 182.0 and 22.0 ppm, corresponding to the bridging acetate. We therefore conclude that the acetate ions in the CdS sample are bound to the surface in a bridging coordination, in agreement with the IR results.

Another indication that the bonding of the acetate on the surface is in a bidentate coordination is the fact that the MAS spectrum of the carboxyl groups shows strong sidebands at low spinning frequencies[16] (not shown). These sideband patterns correspond to a chemical shift anisotropy that is similar to that of a crystalline $CdAc_2 \cdot 2H_2O$ sample. This indicates that the acetate entities are fixed in space and do not rotate around a single oxygen bond, as would be expected in the unidentate coordination.

From these NMR results, we can thus conclude that the Cd atoms on the surface of the CdS nanocrystals are chemically coordinated in four ways: by sulfur oxide ions, hydroxyl groups, O-bonded DMSO, and acetate ion in a bridging form. In addition, large amounts of water are trapped between the particles, enabling the complexation of bulk cadmium acetate with DMSO. A summary of our surface analyses is presented in Table 2.

Reaction Mechanism. To investigate the mechanism of the reaction between the cadmium carboxylates and sulfur in solution, several variations in the reaction procedure were made. At first we checked if the carboxylate ions are essential for the reaction. A DMSO solution of $CdCl_2$ and S was held for 1 h at ca. 120 °C. The UV onset of this solution, after cooling to ambient temperature, was measured at 380 nm. Then sodium acetate was added to the hot solution, and after 35 min the solution changed to a deeper yellow than the original pale yellow of S in hot DMSO. This (cold) solution showed a visible absorption onset at ca. 465 nm. This result shows that, under these conditions, acetate is required for the formation of the CdS nanoparticles. Formation of CdS was also observed when diethylene glycol (a reasonably good solvent for S) was used instead of DMSO, showing that DMSO was not necessary for the reaction.

The reaction mechanism seems to require the mild reducing character of the carboxylates. This is suggested by the fact that formate, a stronger reducing agent than acetate, results in an increase in the reaction rate. To assess this hypothesis, the rest potentials of various DMSO solutions were measured at room temperature. A shift of the solution potential to more reducing values was observed with the addition of $CdAc_2$ and even more with $CdFor_2$, which supports the above role of the carboxylate.

In the electrochemical reduction of Cd^{2+} and S to CdS, two main reaction mechanisms can be considered:[17] the reduction of Cd^{2+} to Cd^0, followed by a chemical reaction of Cd^0 with dissolved S to give CdS, and a reduction of S to S^{2-}, which then reacts with Cd^{2+} to form CdS. The standard potentials of these two reactions are −0.40 V (Cd^{2+}/Cd^0) and −0.48 V (S/S^{2-}).[18] According to the Nernst equation, the actual reduction potential increases with an increase in the ratio of the concentration of the oxidized/reduced species. Because only the oxidized species are nominally present at the start of the reaction, this shift will be large. This may be particularly true for the S/S^{2-} reaction, which, in aqueous solutions, shifts strongly positive with an increase of $[S]/[S^{2-}]$ above unity in a non-Nernstian fashion.[19]

On this basis, although the reduction potentials of the acetate and formate (0.1 and 0.2 eV, respectively[18]) are more positive than the standard potentials of Cd or S, they should be able to reduce these species as long as the concentration of the reduced species remains very low. Because the reduced species (S^{2-} or Cd^0) after formation should react rapidly, this requirement can, in principle, be met.

It is difficult to distinguish between the two possible mechanisms, although reduction of S might appear intuitively more likely. To attempt to gain some insight into this problem, we carried out the same reaction using different metal cations with varying reduction potentials. Pb ($E_0 = -0.12$ V) and Zn ($E_0 = -0.78$ V) were chosen for this purpose. Using the acetate anion of these salts, Pb reacted much more rapidly (immediately at 120 °C) than in the case of Cd, while Zn reacted much slower (at least 140 °C was needed to produce ZnS in 1.5 h, compared to less than 10 min for CdS). These results appear to support the reduction of the metal cation pathway. However, it should be noted that the solubility products of the various sulfides (in water) decrease in the order Zn > Cd > Pb. This means that the amounts of the reduced species required to form the sulfides will decrease in the same order, and therefore the eventual steady-state concentrations of the reduced species will also be lower, leading to a larger Nernst shift from the standard potentials. The solubility product and oxidation potential are thermodynamically related through the free energies of the dissolution reactions (which depend on the free energy, and therefore on the oxidation potential, of the metal ions). Therefore, this interpretation remains ambiguous. It is possible that both mechanisms operate to a greater or lesser extent depending on the reaction conditions. Thus, because of the very large difference between the redox potentials of the acetate and the Zn^{2+} reduction, sulfur reduction is more likely, while in the case of Pb, the opposite may be argued.

(15) Ganapathy, S.; Chacko, V. P.; Bryant, R. G. *J. Chem. Phys.* **1984**, *81*, 661.
(16) Herzfeld, J.; Berger, A. *J. Chem. Phys.* **1980**, *73*, 6021.
(17) Hodes, G. In *Physical Electochemistry*; Rubinstein, I., Ed.; Marcel Dekker: New York, 1995; p 515.
(18) *CRC Handbook of Chemistry and Physics*, 65th ed.; Weast, R. C., CRC Press Inc.: Boca Raton, FL, 1984−1985; p D161.
(19) Allen, P. L.; Hickling, A. *Chem. Ind.* **1954**, *51*, 1558.

A possible third reaction mechanism involves the activation of dissolved sulfur to a sulfide species by a nucleophilic attack or redox disproportionation. This has been discussed by Jiang et al.[20] in the case of the hydrothermal synthesis of tin sulfide species by the reaction of elemental Sn with S. Because $CdCl_2$ and $Cd(ClO_4)_2$ do not react with S, the carboxylate anion would need to play a role in the activation of the sulfur if this mechanism were to occur.

We briefly note for the sake of completeness that the ZnS (sphalerite) crystal size was 2.9 nm, determined by XRD, and that optical absorption measurements resulted in an estimated band gap of 3.85 eV, compared to 3.6 eV for bulk sphalerite ZnS. The room temperature reaction with Pb resulted in a mixture of PbS (with a crystal size of about 30 nm, calculated from XRD spectra) and $Pb_3(CO_3)_2(OH)_2$. At 120 °C, the products were PbS (with a size of 60 nm) and $PbSO_4$.

Extensions of the Preparation Methods

Cadmium Acetate in DMSO. In the course of this study we found that $CdAc_2$ in DMSO, in the absence of S, also forms a precipitate of CdS, although much more slowly than when S is present. A solution of 170 mM $CdAc_2$ in DMSO, kept at room temperature, turned yellow over a period of 7 months with the final UV absorption onset at 480 nm (2.58 V). This same coloration developed over a period of 22 h at 140 °C. At 180 °C, a 100 mM solution of $CdAc_2$ in DMSO gave a 25% yield of CdS in 4 h. XRD of this sample showed the cubic zinc blende phase with a coherence length of 5.9 nm. Similar results were obtained upon ultrasonic treatment of the solution (nominally at room temperature but heated to 70 °C by the ultrasound) with a particularly blue-shifted spectrum of the redissolved precipitate, giving a band gap of ca. 2.9 eV equivalent to a crystal size of 3.0 nm.[21] CdS is formed only slightly, if at all, by sonication of $CdCl_2$ in DMSO (Figure 9a; the absorption here is probably due to decomposition products of the sonicated DMSO, possibly with a small amount of CdS). However, if acetate is added (such as NaAc) to $CdCl_2$ in DMSO, CdS formation does occur, with a strongly blue-shifted spectrum (Figure 9b). We suggest that, during this reaction, DMSO is reduced in the presence of acetate, producing an active form of sulfur that reacts with cadmium. NMR and IR data were used to investigate this reaction.

The spin−echo ^{113}Cd NMR spectrum of the dried sample showed a broad band at the Cd−S chemical shift value that was split into two lines at 692 and 655 ppm (not shown). Both lines are in the range of chemical shifts of fully S-coordinated Cd. The line at 692 ppm can be attributed to Cd atoms fully coordinated to sulfide, while it is shifted away from the peak observed previously at 719 ppm. The origin of this shift can be attributed to the change in the crystallographic phase of the particles. Particularly, this synthetic method results in a cubic phase of CdS, while the samples discussed above were all hexagonal. The cubic phase is known to have a ^{113}Cd chemical shift that is about 20 ppm upfield from that of the hexagonal phase.[22] The second line at 655 ppm can be attributed to surface Cd atoms that are coordinated to decomposed DMSO and which provide a sulfur atom maintaining the full S coordination. An expected Cd−Ac peak is missing in this spectrum.

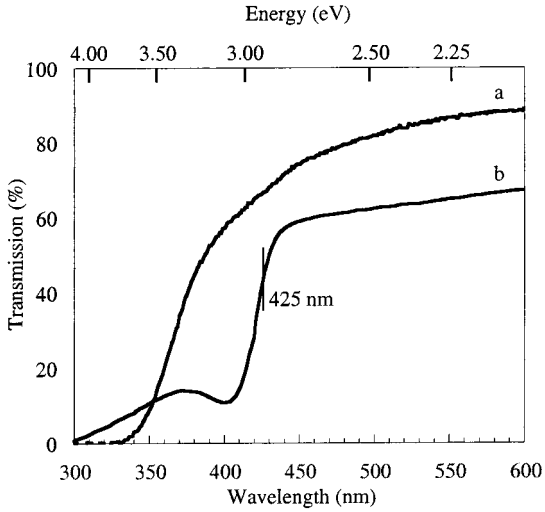

Figure 9. Transmission spectra of (a) a solution of $CdCl_2$ in DMSO treated with a sonic probe for 80 min and (b) after addition of $(CH_3COO)Na$ and sonication for 1 h. The precipitate formed after addition of acetate was washed with methanol and then redissolved in methanol. The gradual absorption in the visible in part a is probably predominantly due to organic decomposition products of the sonicated DMSO.

The ^{13}C spectrum of the CdS sample, obtained from $CdAc_2$ in DMSO, showed a very strong peak at 11.6 ppm in addition to the spectral lines in Figure 8. This chemical shift corresponds to a methyl group that must be assigned to the methyl groups of the decomposed DMSO complex at the surface. An IR spectrum of the same sample indicated that dimethyl sulfide (DMS) is present (IR lines were observed at 4400, 4286, 2981, 2919, and 2835 cm^{-1}). These results suggest that DMS, formed either by acetate-catalyzed disproportionation of DMSO or by direct reduction of DMSO by acetate, reacts with Cd^{2+} in the solution forming a sulfide complex that reacts further and results in CdS. The DMS also efficiently caps the growing crystals, explaining their small size.

Cd(Se,S) Synthesis. The preparation method was extended to mixed selenide−sulfide particles employing mixtures of Se and S in the $CdAc_2$−DMSO solution. Se is much less soluble than S in DMSO but is still sufficient to enable the precipitation reaction. The reaction between $CdAc_2$ and Se in DMSO, without the addition of S, was carried out first. The XRD spectrum of the resulting precipitate showed a shift of the XRD reflection lines to lattice spacings that are smaller than those of pure hexagonal CdSe. This is a result of an incorporation of S atoms from DMSO in the CdSe particles. Assuming Vegard's law (a linear dependence of the lattice parameters with varying composition), the composition was calculated to be $CdS_{0.11}Se_{0.89}$.

Addition of S to the reaction solution resulted in an increase of the S content of the ternary compounds. A nonlinear relationship between the S concentrations in

(20) Jiang, T.; Ozin, G. A.; Bedard, R. L. *Adv. Mater.* **1994**, *6*, 860.
(21) Wang, Y.; Herron, N. *Phys. Rev. B* **1990**, *42*, 7253.
(22) Herron, N.; Wang, Y.; Eckert, H. *J. Am. Chem. Soc.* **1990**, *112*, 1322.

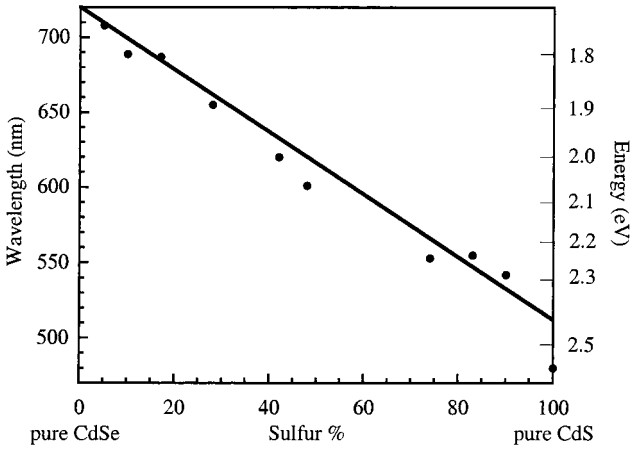

Figure 10. Energy band gaps, estimated from transmission spectra, as a function of the sulfur fraction x in $CdSe_{1-x}S_x$ crystals. The dots are the experimental points, and the solid straight line connects the values of bulk CdSe and CdS.

Table 3. Molar Percentage of Elemental Sulfur [with Respect to the Total Chalcogen (S, Se) Concentration] in the Solution and in the Resulting Precipitate

S in solution	90	80	75	60	50	25	0
S in crystal	74	84	87	42	46	28	11

the solution and in the product was found, as shown in Table 3. Note that S in the crystal may come from the DMSO as well as the dissolved element. The crystal coherence lengths of the CdS_xSe_{1-x} products, measured by XRD, varied between 5 and 10 nm (independent of composition**)**.

Transmission spectra of the redissolved $CdSe_{1-x}S_x$ powders allowed us to determine their band gaps as a function of the sulfur concentration. This dependence is shown in Figure 10. The measured band gaps change linearly with the S concentration. From this we conclude that no appreciable size quantization is observed in these mixed precipitates, in contrast to pure CdS. Small (ca. 0.1 V) changes in the band gaps might have been expected in some cases based on the measured XRD size. Random substitutions of S and Se may lead to loss of X-ray coherence and thus the appearance of smaller than actual size diffraction measurement.

CdSe Synthesis Using Hydrazine. Because Se is only sparingly soluble in DMSO, we looked for a reagent to solubilize Se in order to promote the preparation of CdSe. S is known to dissolve in hydrazine, forming a complex with H_2S in the form of $H_2S.N_2H_4$.[23] Hydrazine, a strong reducing agent, has been used in the past to precipitate metal chalcogenides from aqueous solutions [see ref 24 and references therein].

When hydrazine was added to a 5 mM or more Se solution in DMSO, the color of the solution turned black and the Se dissolved. A filter paper, soaked in a $CuSO_4$ aqueous solution, became black when held above this solution. This blackening is evidence for the formation of H_2Se (reacting with Cu^{2+} to give Cu_xSe). Addition of a Cd salt to the solution caused an immediate change in the color of the solution to yellow and gas formation, presumably N_2.

(23) Welsh, T. W. B.; Broderson, H. J. *J. Am. Chem. Soc.* **1915**, *37*, 825.

(24) Berchenko, M. A.; Belyaev, A. I. *Russ. J. Inorg. Chem.* **1970**, *15*, 1034.

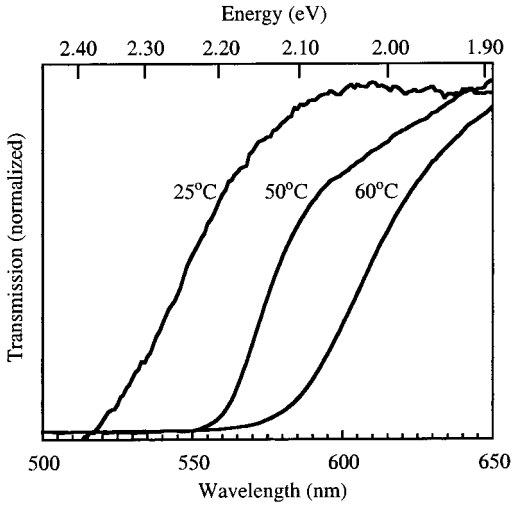

Figure 11. Normalized UV transmission spectra of CdS_xSe_{1-x}, synthesized in the presence of hydrazine at different temperatures. These spectra are obtained from CdS_xSe_{1-x} in the reaction solutions.

The UV spectrum of the solution after this reaction exhibited an increasing blue shift with decreasing preparation temperature, as shown in Figure 11. When the precipitated powder was extracted from the solution, its color changed visually from orange or orange-red to brown. This color remained even after redispersion of the powder in DMSO. This is presumably due to room temperature annealing of the nanocrystals to larger crystals. XRD spectra of the precipitated particles, prepared at different temperatures, showed that they were of the hexagonal phase and had a crystal size of ca. 8 nm. From the XRD peak positions the composition of all of the powders was calculated to be $CdS_{0.17}Se_{0.83}$. Here again, the source of the S atoms was apparently DMSO. For this composition, we expect to have an absorption onset of 1.97 eV, according to the linear correlation described in Figure 10. Approximate band gaps of 2.156, 2.11, and ≈2 eV (the 60 °C spectrum is difficult to analyze because of the relatively heavy scattering) seen in Figure 11 show that quantum size effects occur in these materials in contrast to those produced without hydrazine. Therefore, the hydrazine−Se method leads to smaller crystal size than the equivalent process in the absence of hydrazine. This may be due to capping of CdS_xSe_{1-x} by hydrazine (amines are known to adsorb on CdS) or by DMS, formation by reduction of DMSO by hydrazine, or by a rapid nucleation due to faster reaction.

Summary

In this work we have presented methodologies for the synthesis of CdS and $CdSe_{1-x}S_x$ crystals and characterized their surface chemistry. The CdS crystallites were synthesized by two methods. Starting from $Cd(Ac)_2$ or $Cd(For)_2$ and elemental S solutions in DMSO, the resulting CdS particles showed increasing size quantization effects as the reaction temperature was lowered. When $Cd(For)_2$ was used, the crystal phase was cubic, while in the case of $Cd(Ac)_2$, the CdS crystals were hexagonal. This synthesis was extended to ZnS and PbS. The acetate or formate acted as reducing agents either for elemental S or for metal cations.

The IR and NMR surface investigations of the particles, synthesized from $Cd(Ac)_2$, showed that the acetate is bound to the cadmium on the surface as a bridging complex. The amount of DMSO on the surface is low and exhibits coordination through its oxygen to the surface cadmium. Other chemical terminations of the surface atoms are characterized by bonds between cadmium and hydroxyl ions and by oxidized sulfur atoms.

Nanocrystals of CdS were also synthesized by the reaction of cadmium ions with the DMSO solvent itself, without introducing elemental sulfur, when acetate or formate ions were present in the solution. This reaction was explained by the carboxylate-induced disproportionation or reduction of DMSO to DMS and the reaction of the latter with Cd^{2+}.

Using elemental Se in DMSO, a combination of the two reactions occurred and mixed CdS_xSe_{1-x} particles were formed. The reaction of Cd^{2+} with S, provided by the solvent molecules and in the presence of a reducing agent, competes with the reaction of Cd^{2+} with selenide and resulted in CdS_xSe_{1-x} crystals with different x values. When elemental sulfur was added to this solution, the fraction of S in the crystals could be increased.

The formation of CdS_xSe_{1-x} was also made possible when hydrazine was used as the reducing agent, instead of acetate or formate. In this case the reaction mechanism suggests the formation of a $H_2Se{\cdot}N_2H_4$ complex that subsequently reacts with Cd^{2+}. The hydrazine reduces DMSO to DMS, providing the necessary sulfur for the formation of the mixed crystals. The resulting particles showed stronger quantum size effects when the temperature of the reaction was lowered. When CdS_xSe_{1-x} was precipitated from solution, growth in the particle size occurred because of room temperature annealing.

Acknowledgment. This work was supported by the Israel Ministry of Science, under Contract No. 8461-1-98.

CM0005790